



# Improving Electronic Packaging Manufacturing Through Product and Process-Driven Analysis: A PWB Case Study

**Andrew J. Scholand, Russell S. Peak, and Robert E. Fulton**  
Engineering Information Systems Laboratory, eislab.gatech.edu  
Georgia Institute of Technology  
Atlanta, Georgia 30332

## ABSTRACT

This paper demonstrates how the use of product analysis combined with process data can provide information about the product quality impact of high-level process decisions. A specific case study involving the warpage of two PWB designs as they move through a reflow oven is presented. A new approximate thermal model is derived which analyzes processing rate dependent warpage, an important metric of product quality for ovens with edge support conveyance systems. Agreement between the theoretical model and prior published experimental results was found to be strongly dependent on the precise temperature dependent material property values used, underlining the need to have accurate thermo-mechanical characterizations of PWB constituent materials. A set of property values based on data published in the literature was assembled which provided a fair match to experimental results, giving sufficient confidence to apply the model predictively. For the case study presented, the model predicts a 10% decrease in processing time will increase board warpage by at most 11.5%. This case study illustrates how product analysis can arm production managers with the information they need to make informed, effective decisions which trade off the economic gains realizable by implementing process improvements against the product quality impact of those improvements.

## 1. INTRODUCTION

Managing the manufacturing process in the Electronic Assembly domain is an extremely difficult task. It requires an abstract understanding of the relationship between factors such as design, production system construction and capacity, production control needs, manufacturing process knowledge, and other components of the Product Realization Process (PRP). Solutions often require iteration and consideration of interdisciplinary inter-related factors.

The Electronic Assembly Industry, characterized by highly competitive market pressures and rapid technological advances, further exacerbates the problem of managing manufacturing processes. A time-based competition can be said to exist, where the first company to market with a new product enjoys the most profits. Thus, companies must rapidly change their products and vary production levels to meet fluctuating customer demand. The global nature of the electronics market means that low quality or poorly performing products will lose money, market share, and customer loyalty. Furthermore, in today's business climate the functions of design and manufacture, and their associated expertise, may be spread across geographically and/or organizationally distant entities.

Since process management is so difficult, effective tools are needed to improve the manufacturing stages of the Product Realization Process, and enable Concurrent Engineering and Agile Manufacturing. These tools must explicitly recognize that effectively managing the manufacturing process affects both the quality of goods produced and the manner in which a company satisfies that demand.

This paper documents early progress toward developing a computing infrastructure which links product aware analysis to explicit manufacturing processes, thereby relating product performance characteristics to manufacturing process parameters.

In the sections below we detail the development of an analysis model for dynamic board warpage during solder reflow processing based on an established mechanics of materials model (Classical Lamina Theory) and a first order approximation of the heat transfer through the PWB. Then we review the results of this analysis for two different PWB configurations, to show that the same global process changes can have quite different effects in different products. Finally, we summarize how these analysis results provide a sometimes surprising counterpoint to generic industrial engineering process improvement suggestions.

## 2. BACKGROUND

### 2.1 Classical Lamina Theory

Classical Lamina Theory (CLT) analyzes the behavior of fibrous composites by idealizing the composite as a structure consisting of layers (or lamina) with the following characteristics:

- Each layer is assumed to be homogeneous, elastic, and orthotropic
- Each layer is assumed to be in a state of plane stress
- Only certain displacements are assumed to occur- Kirchhoff assumptions
  - Normals to the midplane remain straight and normal to the deformed midplane
  - Normals do not change length
- Each layer is perfectly bonded to adjacent layers (no slippage between the plies)
- Each layer is constant in thickness

The fundamental equations of lamination theory relate in-plane forces (such as those developed by constraining thermal expansion) and bending moments per unit length to midplane strains and curvatures of the laminates. These equations reveal the effect of layer material properties, layer fiber orientations, layer thickness, and stacking sequence of the layers on the laminated composite deformation response to a given load.

### 2.2 Laminae Stiffness

Consider a laminae with principal coordinate axes at an angle to global X-Y coordinate axes as shown below:

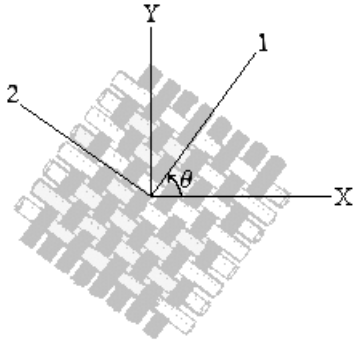


Figure 2.2-1: Woven Laminae with 2 coordinate systems

The principle material coordinates are aligned along the warp/fill directions when modeling woven fiber composites such as FR-4 epoxy glass. We can write constitutive stress-strain relations in the principal material coordinates since each individual layer is assumed to be homogeneous, elastic, and orthotropic:

$$\sigma_i = Q_{ij} \varepsilon_j \quad i, j = 1, 2, \dots, 6 \quad (1)$$

The matrix  $Q$  is known as the stiffness matrix, and for plane stress its terms are:

$$Q_{11} = \frac{E_1}{1 - \nu_{12}\nu_{21}} \quad (2)$$

$$Q_{22} = \frac{E_2}{1 - \nu_{12}\nu_{21}} \quad (3)$$

$$Q_{12} = \frac{\nu_{21}E_2}{1 - \nu_{12}\nu_{21}} = \frac{\nu_{12}E_1}{1 - \nu_{12}\nu_{21}} \quad (4)$$

$$Q_{66} = G_{12} \quad (5)$$

$$\text{Zero elsewhere} \quad (6)$$

$E_1, E_2, \nu_{12}, \nu_{21}, G_{12}$  are the elastic engineering constants of the individual lamina in its principal material directions. To map from the principal coordinate system to the global X-Y coordinate system, a transformation tensor must be applied to  $Q$ :

$$[\bar{Q}] = [T_1]^{-1} [Q] [T_2] \quad (7)$$

$$T_1 = \begin{bmatrix} \cos^2\theta & \sin^2\theta & 2\cos\theta\sin\theta \\ \sin^2\theta & \cos^2\theta & -2\cos\theta\sin\theta \\ -\cos\theta\sin\theta & \cos\theta\sin\theta & \cos^2\theta - \sin^2\theta \end{bmatrix} \quad (8)$$

$$T_2 = \begin{bmatrix} \cos^2\theta & \sin^2\theta & \cos\theta\sin\theta \\ \sin^2\theta & \cos^2\theta & -\cos\theta\sin\theta \\ -2\cos\theta\sin\theta & 2\cos\theta\sin\theta & \cos^2\theta - \sin^2\theta \end{bmatrix} \quad (9)$$

Positive  $\theta$  is measured from the positive x axis to the positive 1 axis, as shown in Figure 2.2-1.

### 2.3 Laminae Deformation

Certain assumptions are made about the deformation of the laminate as mentioned in Section 2.1 (the Kirchhoff-Love hypotheses for thin plates and shells). Namely we ignore transverse shear strains and normal strain in the z direction:

$$\gamma_{xz} = \gamma_{yz} = \varepsilon_z = 0 \quad (10)$$

For small strains and using linearized theory of elasticity, the strains  $\{\varepsilon\}_x$  in the global X-Y coordinate system at any distance z from the midplane are written as:

$$\begin{Bmatrix} \varepsilon_x \\ \varepsilon_y \\ \gamma_{xy} \end{Bmatrix} = \begin{Bmatrix} \varepsilon_x^0 \\ \varepsilon_y^0 \\ \gamma_{xy}^0 \end{Bmatrix} + z \cdot \begin{Bmatrix} \kappa_x \\ \kappa_y \\ \kappa_{xy} \end{Bmatrix} \quad (11)$$

where the zero superscript indicates these strains are the midplane strains and  $\{\kappa\}_x$  are the plate curvatures.

## 2.4 Lamina Forces and Moments

The stresses at a specific location are obtained by plugging the strain equation into the constitutive equation. Thus, for each layer  $k$ ,

$$\begin{Bmatrix} \sigma_x \\ \sigma_y \\ \tau_{xy} \end{Bmatrix}_{(k)} = [\bar{Q}]_{(k)} \cdot \begin{Bmatrix} \epsilon_x^0 \\ \epsilon_y^0 \\ \gamma_{xy}^0 \end{Bmatrix} + z_{(k)} \cdot \begin{Bmatrix} \kappa_x \\ \kappa_y \\ \kappa_{xy} \end{Bmatrix} \quad (12)$$

The forces  $\{N\}$  and moments  $\{M\}$  per unit length must be obtained by integrating the stresses over the thickness of each laminate:

$$\{N\} = \int_{-\frac{H}{2}}^{+\frac{H}{2}} \begin{Bmatrix} \sigma_x \\ \sigma_y \\ \tau_{xy} \end{Bmatrix} \cdot dz = \sum_{k=1}^N \int_{h_{k-1}}^{h_k} \begin{Bmatrix} \sigma_x \\ \sigma_y \\ \tau_{xy} \end{Bmatrix}_{(k)} dz \quad (13)$$

$$\{M\} = \int_{-\frac{H}{2}}^{+\frac{H}{2}} z \cdot \begin{Bmatrix} \sigma_x \\ \sigma_y \\ \tau_{xy} \end{Bmatrix} \cdot dz = \sum_{k=1}^N \int_{h_{k-1}}^{h_k} z_k \begin{Bmatrix} \sigma_x \\ \sigma_y \\ \tau_{xy} \end{Bmatrix}_{(k)} dz \quad (14)$$

The definition of the various integration variables in Equations 13 and 14 is best described by the figure below.

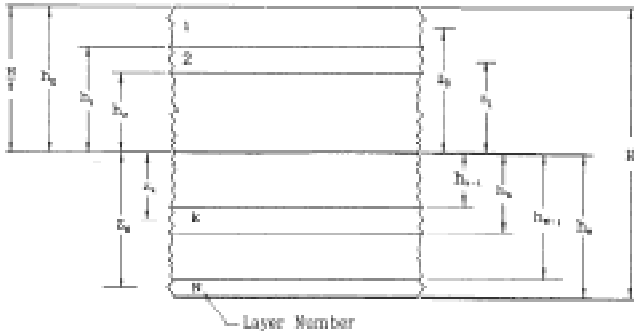


Figure 2.4-1: Definition of various measurements of the lamina stack

## 2.5 CLT Equations

Integration of the force and moment equations provides the fundamental equations of lamination theory, which can be written in matrix form. In the case of applied thermal loads, the thermal force and thermal moment matrices must be included:

$$\begin{Bmatrix} N \\ M \end{Bmatrix} = \begin{bmatrix} A & B \\ B & D \end{bmatrix} \begin{Bmatrix} \epsilon^0 \\ \kappa \end{Bmatrix} - \begin{Bmatrix} N^T \\ M^T \end{Bmatrix} \quad (15)$$

where

$$[A] = \sum_{k=1}^N [\bar{Q}]_{(k)} (h_k - h_{k-1}) \quad (16)$$

$$[B] = \frac{1}{2} \sum_{k=1}^N [\bar{Q}]_{(k)} (h_k^2 - h_{k-1}^2) \quad (17)$$

$$[D] = \frac{1}{3} \sum_{k=1}^N [\bar{Q}]_{(k)} (h_k^3 - h_{k-1}^3) \quad (18)$$

$$[N^T] = \sum_{k=1}^N \int_{h_{k-1}}^{h_k} [\bar{Q}]_{(k)} \begin{Bmatrix} \alpha_x \\ \alpha_y \\ 0 \end{Bmatrix}_{(k)} \Delta T_k \cdot dz \quad (19)$$

$$[M^T] = \sum_{k=1}^N \int_{h_{k-1}}^{h_k} [\bar{Q}]_{(k)} \begin{Bmatrix} \alpha_x \\ \alpha_y \\ 0 \end{Bmatrix}_{(k)} \Delta T_k \cdot z_k \cdot dz \quad (20)$$

If the applied external forces and moments are zero, then the equation becomes:

$$\begin{Bmatrix} N^T \\ M^T \end{Bmatrix} = \begin{bmatrix} A & B \\ B & D \end{bmatrix} \begin{Bmatrix} \epsilon^0 \\ \kappa \end{Bmatrix} \quad (21)$$

which can be solved for the midplane displacements  $\epsilon^0$  and  $\kappa$ . Once these are known, a plate-wide displacement field (warpage) can be computed for a square plate with side of length  $a$ :

$$w(x, y) = \frac{a}{2} (\kappa_x x + \kappa_y y) - \frac{1}{2} (\kappa_x x^2 + \kappa_y y^2 + \kappa_{xy} xy) \quad (22)$$

Note that this equation measures warpage from the plane determined by 3 corners of the plate- (0,0), (a,0), and (0,a).

## 3. DYNAMIC THERMAL MODELING

The above section described how Classical Laminate Theory will provide an assessment of the warpage a laminate will experience upon a given temperature excursion from a stress-free state, where each layer may have a unique temperature. If each layer is in fact at a different temperature, this thermal gradient can create greater warpage than will be experienced due to uniform heating, especially in the case of symmetric layups. A dynamic thermal model is needed to correctly assign various layer temperatures to match the thermal loading experienced by a PWB during manufacturing operations.

We argue that the thermal field can be roughly approximated with the following. We presume firstly that the temperature-time profile of the PWB top surface (only) is known<sup>1</sup>, and can be approximated with a polynomial function of time. Second, we make the gross simplification that heat transfer from the bottom of the PWB is negligible. Third, we assume the length and width of the PWB are much greater than its thickness. Thus, the problem of determining the temperature gradients through the PWB simplifies to one-dimensional unsteady conduction. We shall attack this problem in two parts. First, by treating the PWB as a lumped mass, we can determine the total transient heat that instantaneously flows in or out of the PWB. Then, using a thermal resistance model, we can identify the through-

<sup>1</sup> This data is gathered experimentally, by sending a PWB with temperature gauges through the process to be profiled.

thickness temperature profile of the PWB that corresponds to this heat flow.

Oien (1976) has shown that the Biot number for multilayer circuit boards being heated by radiative, convective, and forced convective environments in air is much less than 1. As long as the Biot number is small compared to unity, the thermal gradients within the PWB are small. For this case, it is a reasonable first order approximation to model the PWB as a lumped system at a single internal, uniform temperature inside an insulating jacket.

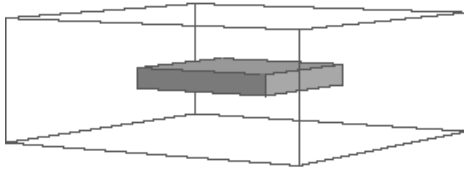


Figure 2.5-1: Approximate Physical Model

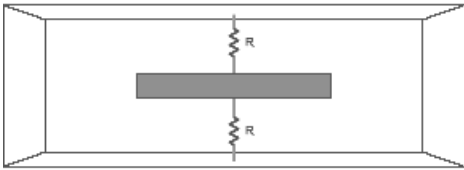


Figure 2.5-2: Thermodynamic Analysis Model

Applying a first law thermodynamic analysis to the thermal conduction in this system, we find that:

$$\frac{d[T_0(t)]}{dt} = \frac{1}{cmR} (T_L(t) - T_0(t)) \quad (23)$$

where

- $T_0(t)$  is the inner lumped temperature of the PWB
- $T_L(t)$  is the temperature of the outer surface
- $c$  is the averaged specific heat of the PWB, assumed to be constant over temperature
- $m$  is the total lumped mass of the PWB
- $R$  is the total thermal resistance from the PWB surface to the lumped-mass center

This equation is a linear differential equation, and if the external temperature  $T_L(t)$  is a known polynomial, an exact solution can be obtained. Assuming the temperature profile is described by a quintic, the solution is:

$$\begin{aligned} T_0(t) = & T_L(t) - cmR \cdot \frac{d[T_L(t)]}{dt} + (cmR)^2 \cdot \frac{d^2[T_L(t)]}{dt^2} \\ & - (cmR)^3 \cdot \frac{d^3[T_L(t)]}{dt^3} + (cmR)^4 \cdot \frac{d^4[T_L(t)]}{dt^4} \\ & - (cmR)^5 \cdot \frac{d^5[T_L(t)]}{dt^5} - \frac{c_2}{e^{cmR}} \end{aligned} \quad (24)$$

The unknown constant of integration  $c_2$  must be determined from boundary conditions. It represents the initial conditions of the problem (thermal equilibrium of the PWB at time  $t=0$ ), and its effects die out over time.

The instantaneous difference between the temperatures of the inner and outer sides of the insulating jacket will drive heat through the thermal resistance of the jacket:

$$q(t) = \frac{T_0(t) - T_L(t)}{R} \quad (25)$$

We now assume the heat transfer calculated for the lumped model holds true in the multilayer structure. If adjacent layers in the PWB have the same temperature at their interfaces (i.e. that thermal contact resistance is zero), the entire temperature profile through the PWB can be established for any time  $t$  by evaluating

$$T_i(t) = R_i \cdot q(t) + T_0(t) \quad (26)$$

where

$T_i$  is the temperature of the  $i$ th layer in the PWB stack, a function of time  $t$

$R_i$  is the thermal resistance through the  $i$ th layer in the PWB stack

$q$  is the heat flowing through all layers, a function of time  $t$

Thus, temperature gradients through the PWB are transient, linear, and based on the lumped thermal model. These temperature-time profiles can now be combined with Classical Lamina Theory constitutive equations to yield the gross thermo-elastic behavior of the PWB.

## 4. CASE STUDY

To illustrate how global process variables relate explicitly to product-specific measures of quality, a case study will be discussed which illustrates how a global process variable (processing time) relates to a quality measure (PWB warpage). In on-going research, we are developing a CAE framework that allows these relationships to be explicitly explored and understood in an automated manner.

### 4.1 Product Data

The PWBs to be utilized for this case study are based on samples described in Stiteler and Ume (1997) and Stiteler et. al. (1996), illustrated below.

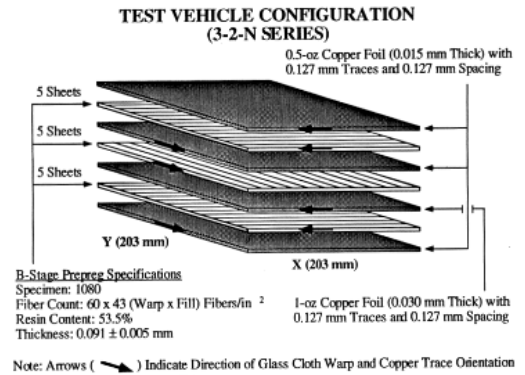
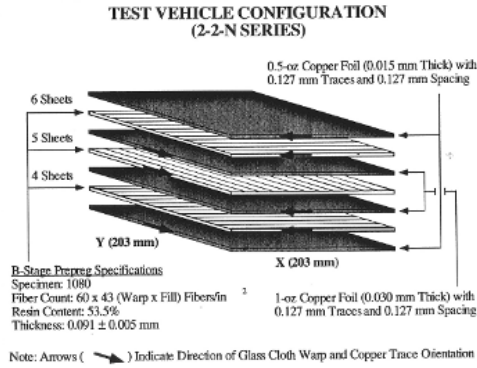


Figure 4.1-1: 3-2-N PWB Layup Data



**Figure 4.1-2:** 2-2-N PWB Layout Data

These PWBs are physical simplifications of real PWBs, in that the copper traces are unidirectional and run the full length of the board. However, CLT analyses require substantial information concerning the product and production processes, which Stiteler et. al. have provided. In addition, they have published experimental measurements of many of the parameters of interest, which provide a useful real world accuracy check.

## 4.2 Material Data

Temperature dependent material properties are surprisingly hard to find in the literature, given that analyses based on temperature-dependent values often differ substantially from those based on constant value assumptions (Fu and Ume, 1995).

Most of the published sources for temperature-dependent data on FR-4 fiberglass-epoxy woven composites are plated through hole analyses where the X and Y directions are presumed to have equal material properties to permit axisymmetric analyses. For the purposes of this model, Young's Modulus and Shear Modulus data from Barker et. al. are assumed to be an average of these in-plane properties. Warp and fill material properties have been approximated by adding or subtracting a constant factor respectively to Barker's data, and then fitting a curve through those points. These equations are listed below.

Unlike plated through hole analysis (Wu et. al., 1993), warpage behavior is very dependent on the exact behavior of the coefficient of thermal expansion (CTE) around the glass transition ( $T_g$ ) temperature of FR-4. Phenomenologically, the CTE increases slightly with temperature up until shortly before the  $T_g$ , then rapidly drops to a relatively constant value above  $T_g$ . Vecchio and Hertzberg (1986) provide CTE data for each material axis up to just below the transition temperature of FR-4. A constant value for the CTE in each direction above the glass transition temperature was chosen in agreement with other published values (e.g. Dasgupta and Ramappan [1995]), and transitions between these data points are simple linear interpolations. Selection of the appropriate 'switch' temperatures for each region was found to profoundly affect results, however, and a degree of trial and error was required to arrive at the values shown below.

$$E_1 = 1.6523 \cdot 10^{-6} T^3 - 0.00065695 T^2 + 0.035105 T + 22.09 \text{ GPa}$$

$$E_2 = 1.6523 \cdot 10^{-6} T^3 - 0.00065695 T^2 + 0.035105 T + 21.7 \text{ GPa}$$

$$G = 1.3831 \cdot 10^{-7} T^3 - 5.5756 \cdot 10^{-5} T^2 + 0.0046092 T + 0.539 \text{ GPa}$$

$$\nu_{12} = 0.16$$

$$C_p = 840 \text{ J/kg } ^\circ\text{C}$$

$$k = 0.26 \text{ W/m } ^\circ\text{C}$$

$$\rho = 1671.3 \text{ kg/m}^3$$

$$\alpha_1 = 0.043182 * (T - 25^\circ\text{C}) + 17.5 \text{ ppm/}^\circ\text{C if } T < 113^\circ\text{C}$$

$$= 21.3 - 0.43182 * (T - 113^\circ\text{C}) \text{ ppm/}^\circ\text{C if } 113^\circ\text{C} \leq T < 135^\circ\text{C}$$

$$= 11.8 \text{ ppm/}^\circ\text{C if } T \geq 135^\circ\text{C}$$

$$\alpha_2 = 0.057955 * (T - 25^\circ\text{C}) + 14.7 \text{ ppm/}^\circ\text{C if } T < 113^\circ\text{C}$$

$$= 19.8 - 0.44545 * (T - 113^\circ\text{C}) \text{ ppm/}^\circ\text{C if } 113^\circ\text{C} \leq T < 135^\circ\text{C}$$

$$= 10 \text{ ppm/}^\circ\text{C if } T \geq 135^\circ\text{C}$$

**Table 1:** Material Properties used to model FR-4

The copper traces on the PWB must also be modeled in some fashion. These particular PWBs were fabricated expressly so that the copper layers could be modeled as continuous fibrous composites with definite 'warp' and 'fill' directions. However, how such an approach can be extended to model real-world circuit layers, where no discernable pattern may exist, is unclear. We adopted an intermediate approach, where orthotropic material properties are calculated using standard 'rule of mixtures' equations (Dowling, 1993) but then averaged together to produce an isotropic layer. Thus, the modeling of a circuit layer requires only an estimate of the volume of copper in the layer. Copper Young's Modulus data were taken from Ume and Fu (1995), while the epoxy data were taken from Wu et. al. (1993). The following isotropic elastic properties were used for the copper and epoxy:

$$E = 2.1215 \cdot 10^{-7} T^4 - 1.061 \cdot 10^{-6} T^3 + 0.0171 T^2 - 1.197 T + 126 \text{ GPa}$$

$$\nu_{12} = 0.3$$

$$C_p = 384 \text{ J/kg } ^\circ\text{C}$$

$$k = 380.62 \text{ W/m } ^\circ\text{C}$$

$$\rho = 8940 \text{ kg/m}^3$$

$$\alpha = 17 \text{ ppm/}^\circ\text{C}$$

**Table 2:** Material Properties used to model Copper

$$E = 2.4 \text{ GPa if } T < 125^\circ\text{C}$$

$$= 0.07 \text{ GPa if } T \geq 125^\circ\text{C}$$

$$\nu_{12} = 0.37 \text{ if } T < 125^\circ\text{C}$$

$$= 0.49 \text{ if } T \geq 125^\circ\text{C}$$

$$\alpha = 60 \text{ ppm/}^\circ\text{C if } T < 125^\circ\text{C}$$

$$= 90 \text{ ppm/}^\circ\text{C if } T \geq 125^\circ\text{C}$$

**Table 3:** Material Properties used to model Epoxy

The ‘rule of mixtures’ equations were also applied to the outer circuit layers (which are not surrounded by epoxy like the inner circuit layers) by assuming a ‘virtual’ matrix material with all elastic constants set to zero.

### 4.3 Process Data

Stiteler and Ume (1997) also provide the temperature-time profile of the top side of the PWB during reflow. The profiles shown below are a slight modification of their profile, in that a temperature decrease is imposed where the PWB passes under the exhaust flue of the oven. This increasing, then decreasing temperature profile is often seen in practice, and leads to some interesting board behavior, as the bottom layers of the board are sometimes hotter than the upper layers. A quintic polynomial has been fitted to the first 400 seconds of this data, and is shown in Figure 4.3-1. The effects of ‘expediting’ this board to reduce processing time are modeled by the temperature-time profile shown in Figure 4.3-2, where the overall time in the oven is reduced to 360 seconds but the temperature excursions are held constant.

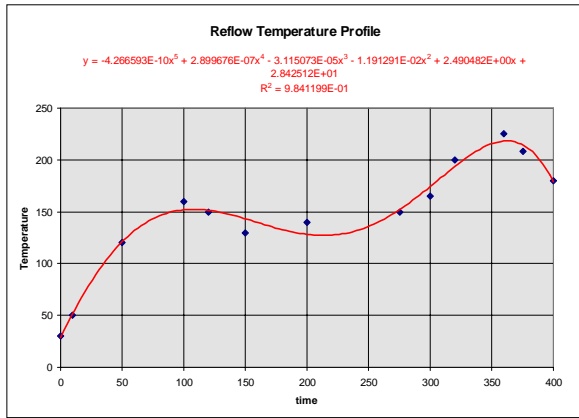


Figure 4.3-1: Standard reflow temperature profile

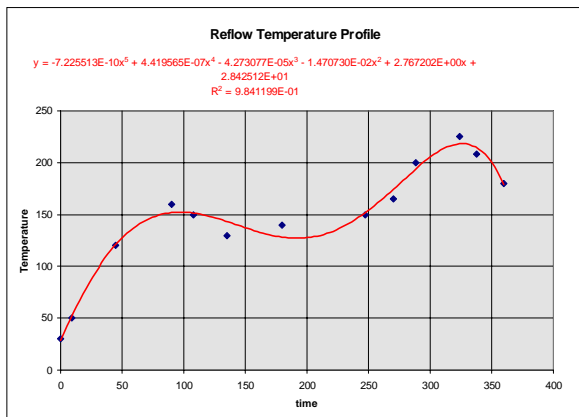


Figure 4.3-2: Expedited reflow temperature profile

### 4.4 Model Validation

The first portion of the model to evaluate is the thermal modeling portion, since several assumptions were made in deriving it. Stiteler (1997) has published temperature profiles measured by thermocouples on the top and bottom of the 3-2-N layup, showing that when the top surface of the board is between 160°C and 220°C, the maximum temperature difference between the upper and lower surface of the board is 16°C. The thermal model presented here predicts a thermal gradient of 11°C when following the same portion of Stiteler’s temperature profile. While some of the differences between the experimental and theoretical results may be accounted for by thermal contact resistance between the PWB and the thermocouples and other experimental error, the majority of the discrepancy is due to the first-order approximate nature of the analytical model itself. In particular, the assumption of constant specific heat ( $C_p$ ) for FR-4 versus temperature has been shown to be inaccurate (Sarvar and Conway, 1996). In fact,  $C_p$  increases almost linearly with temperature up to 120°C. Thus, because  $C_p$  is underestimated at temperatures above room temperature, the amount of heat flowing into the PWB is also underestimated, leading to lower temperature gradients through the board.

Next we consider the gross mechanical warpage. Stiteler and Ume (1997) have provided warpage measurements for the 2-2-N layup at 9 positions (four outer corners, midpoints of the four outer sides, and the center) at several temperatures. This warpage is measured relative to the specimen’s warpage at room temperature. For the purposes of this study, two temperatures were selected for comparing the experimental and theoretical warpage- 120°C during heating, and 216°C during heating. Heating cycle temperatures were selected rather than cooling temperatures since the experimental equipment can better reproduce heat-up ramps than cool-down ramps, and the theoretical polynomial curve fit to the temperature-time profile is better on the heating cycle. To allow direct comparison to the theoretically calculated warpage, a plane was fitted through three corners of the warped PWB, and the published displacements were adjusted to values measured from this plane. Since these figures differ substantially from those published by Stiteler and Ume, they are reproduced overleaf.

Examination of these warpage measurements reveals that the lamina principal directions are not in exact alignment with the global coordinate system, since the warpage in each quadrant of the board is different. Boards with material axes in line with global axes (a  $\theta$  equal to a multiple of  $\pi/2$ ) exhibit warpage with symmetry about the global axes. Since the 2-2-N layup calls for all lamina principal directions to be aligned at 0 or 90 degrees, there is obviously a manufacturing-induced non-uniformity in the samples. However, the warpage at the center of the board is relatively unaffected by small misalignments in the plies, and so the center point warpage (labeled CENTER CENTER in Table 4 and Table 6 overleaf) is a relatively good comparison point for theoretical warpage (perfect ply alignment) and experimental warpage (small unknown random ply mis-alignments). Results of the theoretical model at each of the two comparison temperatures are shown in Table 5 and Table 7 overleaf.

There are some differences between the theoretical and experimental warpage. One reason has been stated above, namely that the approximate thermal model underestimates the temperature gradient through the PWB, so that warpage is less severe in the predicted model. In addition, the experimental specimens are subjected to gravitational body forces and concentrated reaction forces

TOP LEFT	TOP CENTER	TOP RIGHT	CENTER LEFT	CENTER CENTER	CENTER RIGHT	BOTTOM LEFT	BOTTOM CENTER	BOTTOM RIGHT
0	-1.08	-0.51	-1.08	-2.16	-0.70	0	-0.32	0
0	-1.08	-0.51	-0.83	-2.16	-0.83	0	-0.32	0

**Table 4:** Adjusted values of Stiteler's Experimental 120°C (Heating Cycle) 2-2-N warpage in millimeters

TOP LEFT	TOP CENTER	TOP RIGHT	CENTER LEFT	CENTER CENTER	CENTER RIGHT	BOTTOM LEFT	BOTTOM CENTER	BOTTOM RIGHT
0	-1.15	0	-0.85	-2.00	-0.85	0	-1.15	0

**Table 5:** 2-2-N Predicted Results (Perfect Ply Alignment) in millimeters at 120°C Heating Cycle Warpage

TOP LEFT	TOP CENTER	TOP RIGHT	CENTER LEFT	CENTER CENTER	CENTER RIGHT	BOTTOM LEFT	BOTTOM CENTER	BOTTOM RIGHT
0	-0.44	0	-0.63	-1.21	0.13	0	0.32	0
0	-0.32	0.25	-0.63	-1.08	0.25	0	0.44	0

**Table 6:** Adjusted values of Stiteler's Experimental 216°C (Heating Cycle) 2-2-N warpage in millimeters

TOP LEFT	TOP CENTER	TOP RIGHT	CENTER LEFT	CENTER CENTER	CENTER RIGHT	BOTTOM LEFT	BOTTOM CENTER	BOTTOM RIGHT
0	-0.82	0	-0.18	-1.00	-0.18	0	-0.82	0

**Table 7:** 2-2-N Predicted Results (Perfect Ply Alignment) in millimeters at 216°C Heating Cycle Warpage

along two of the edges. These forces allow the unsupported center of the PWB to sag slightly, increasing the bowl like warpage seen here, especially at the elevated temperatures where the materials' stiffness is lower. Given these differences, and other possible warpage factors that are not accounted for, the proposed theoretical model is reasonably accurate.

With a degree of confidence in the validity of the model as a first order approximation, then, we can examine the effect of decreasing processing time on product quality.

#### 4.5 Predicted Effects of Manufacturing Level Changes

As mentioned in Section 4.3, a global decision can be made to 'expedite' a manufacturing process to increase throughput or reduce work-in-process inventory levels. Expediting a solder reflow process would mean at a minimum increasing the conveyor speed at which products move through the oven. By applying the resulting differing temperature-time profiles to the specific products that will be soldered, a measure of the impact of the global decision on one aspect of product quality can be made.

The figure below is the warpage at the center of the 2-2-N board experienced at the 'standard' conveyor speed and at the expedited speed.

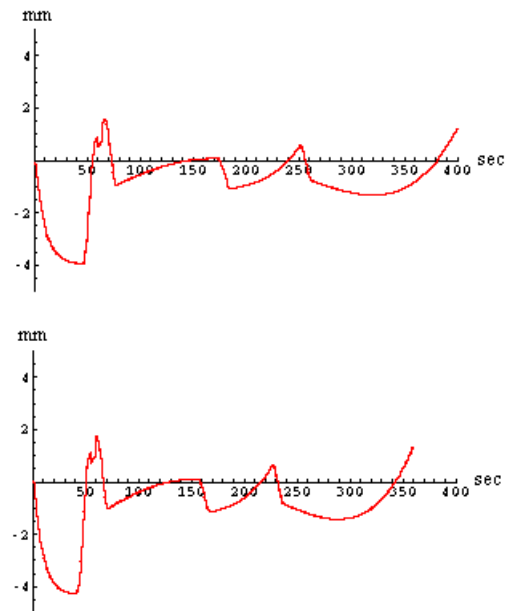


**Figure 4.5-1:** Center warpage of 2-2-N PWB under standard (top) and expedited (bottom) conditions

We can examine the same two global options on a different product, this time the 3-2-N boards. Once again, the standard profile is on the top, and the expedited profile is on the bottom.

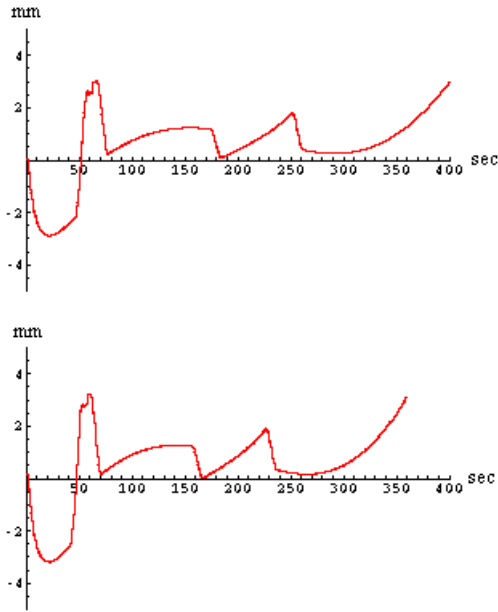


**Figure 4.5-2:** Center warpage of 3-2-N PWB under standard (top) and expedited (bottom) conditions

In tabular form, the maximum and minimum warpages are:

	2-2-N		3-2-N	
	Maximum	Minimum	Maximum	Minimum
Standard	+1.57 mm	-3.94 mm	+3.02 mm	-2.89 mm
Expedited	+1.75 mm	-4.25 mm	+3.24 mm	-3.19 mm
Percent change	11.5%	7.9%	7.3%	10.4%

**Table 8:** Product Quality Effect of Expediting on Two Different Products

Comparing the maximum warpage under the two global processing options, we see that the warpage experienced by a 2-2-N board increased by 11.5% and the warpage experienced by a 3-2-N board increased by 10.4% when processed 10% faster through the reflow oven!

The relatively unsmooth nature of the warpage plot can be explained by the relatively simple material models discussed in Section 4.2. For comparison, the predicted warpage of the 2-2-N layout is shown below under standard processing conditions when constant material properties are used.

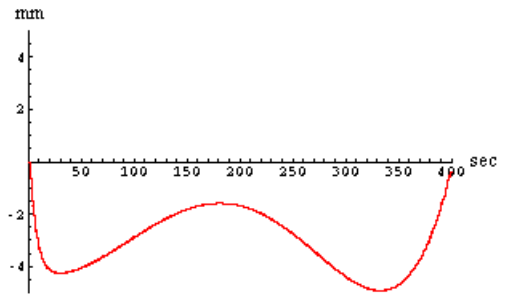


**Figure 4.5-3:** Centerline warpage of 2-2-N PWB assuming constant material properties

Although the graph is much smoother, notice that there is a substantial error in assuming non-temperature dependent material properties. Such temperature independent plots are much quicker to generate, however, requiring only 30 minutes on a 133MHz Pentium versus 4 hours per plot for the temperature dependent plots.

## 5. DISCUSSION AND CONCLUSION

Standard Industrial Engineering metric generally indicate that repeatable, shorter processing times are better, since they lead to greater throughput and lower work-in-progress inventories. In this specific case, however, expediting the products through the reflow process had adverse affects on one specific measure of product quality, board warpage. The degree to which the same throughput improvement affected product quality differed for the two products analyzed, however. To make informed, effective decisions that trade off the economic gains realizable by implementing process improvements against the product quality impact of those improvements, analyses must be performed. The key to leveraging this decision-critical information contained in analysis models is to

1. Identify the important ‘figures of merit’ for a product
2. Identify what analysis models are necessary to provide estimates of these figures of merit to a sufficient degree of accuracy given the computational resources available
3. Identify how analysis model variables and global processing variables interrelate
4. Implement these analysis models in a framework which aids their application, including the automatic extraction of product and process details from neutral standards-based data files such as STEP.

This paper has illustrated how a warpage analysis model can illuminate the connections between global process variables and individual measures of product quality, thereby covering items 1, 2, and 3 on the list above. We are currently working on the fourth item and other logical applications of such a framework.

## 6. REFERENCES

Barker, D., Pecht, M., Dasgupta, A., and Naqui, S. (1991) “Transient Thermal Stress Analysis of a Plated Through Hole Subjected to Wave Soldering,” *ASME Journal of Electronic Packaging*, Vol. 114, No. 2, pp. 149-155.

Dasgupta, A., and Ramappan, V. (1995) "Simulation of the Influence of Manufacturing Quality on the Reliability of Vias," *ASME Journal of Electronic Packaging*, Vol. 117, pp. 141-146.

Dowling, Norman E. (1993) *Mechanical Behavior of Materials*, Prentice Hall, Inc.

Fu, C., and Ume, C. (1995) "Characterizing the Temperature Dependence of Electronic Packaging Material Properties," *JOM*, Vol. 47, No. 6, pp. 31-35.

Karalekas, D., Daniel, I.M., and Gotro, J.T., (1987) "The Influence of Lamination Parameters on Warpage of Woven-Glass/Epoxy Laminates", ANTEC 1987, pp. 339-341.

Peak, R. S.; Fulton, R. E.; Nishigaki, I.; Okamoto, N., (1995) "Integrating Engineering Design and Analysis Using a Multi- Representation Approach", *Engineering with Computers*, to appear (submitted March 1995).

Peak, R. S.; Scholand, A. J; Fulton, R. E., (1996) "On the Routinization of Analysis for Physical Design. Application of CAE/CAD to Electronic Systems", EEP-Vol.18, Agonafar, D., et al., eds., 1996 ASME Intl. Mech. Engr. Congress & Expo., Atlanta, pp. 73-82.

Peak, R. S., (1996) "A Survey of Engineering Framework Technology with Applications to Computer Aided Engineering", 6th Intl. Conference, Flexible Automation & Intelligent Manufacturing (FAIM 96), May 13-15, 1996, Atlanta, pp. 47-56.

Sarvar, Farhad and Conway, Paul P. (1996) "Effective Transient Process Modeling of the Reflow Soldering of Printed Circuit Assemblies," 1996 InterSociety Conference on Thermal Phenomena, pp. 195-202.

Stiteler, Michael R., (1996) "An Automated System for Measuring PWB/PWA Warpage During Simulation of the Infrared Reflow and Wave Soldering Processes, and During Operational Thermal Cycling", Masters Thesis, Georgia Institute of Technology, Atlanta.

Stiteler, Michael R., and Ume, Charles, (1997) "System for Real-Time Measurement of Thermally Induced PWB/PWA Warpage," *Journal of Electronic Packaging*, Vol. 119, March 1997, pp. 1-7.

Stiteler, Michael R., Ume, Charles, and Leutz, Brian, (1996) "In-Process Board Warpage Measurement in a Lab Scale Wave Soldering Oven," 1996 Electronic Components and Technology Conference, IEEE, May 1996, pp. 247- 254.

Tamburini, D. R., Peak, R. S., and Fulton R. E. (1997) "Driving PWA Thermomechanical Analysis from STEP AP210 Product Models." *1997 ASME International Mechanical Engineering Congress and Exposition*, To be published.

Vecchio, K. S., and Hertzberg, R. W. (1986) "Analysis of Long Term Reliability of Plated Through Holes in Multilayer Interconnection Board. Part A: Stress Analysis & Material Characterization," *Microelectronics Reliability*, Vol. 26, No. 4, pp. 715-732.

Wu, T. Y., Guo, Y., and Chen, W. T. (1993) "Thermal Mechanical Strain Characterization for Printed Wiring Boards," *IBM Journal of Research and Development*, Vol. 37, No. 5, pp. 621-634.

Zewi, I.G., Daniel, I.M., and Gotro, J.T., (1987) "Residual Stresses and Warpage in Woven-Glass/Epoxy Laminates," *Experimental Mechanics*, March 1987, pp. 44-50.